Prepared for submission to JHEP

Charmed particle production in tau-neutrino CC interaction detected by OPERA

OPERA collaboration

Abstract:

A peculiar event topology with two secondary decay vertices compatible with short lived particles was found in the analysis of neutrino interactions in the OPERA target. Only few neutrino interactions can yield two heavy particles in the final state: ν_τ CC interaction with charm production or ν NC interaction with $c\bar{c}$ pair production.

A dedicated analysis was set-up to identify the underlying process. A new Monte Carlo was developed and several innovative procedures were introduced in the kinematic reconstruction. Multivariate analysis techniques were used to achieve an optimal signal to background separation.

Most likely this event is a ν_τ CC interaction with charm production. The significance of this observation is 3.5 σ.

Contents

1 Introduction **1**

2 The OPERA experiment **2**
2.1 The apparatus 2
2.2 Data taking and event reconstruction 2

3 Event 1114301850 **4**
3.1 Data acquisition, event building and reconstruction 5
3.2 Kinematics 7

4 Event analysis **10**

5 Significance **13**

6 Conclusions **14**

1 Introduction

Charmed hadron production in neutrino interactions have been studied in two ways: dilepton searches in calorimeter detectors [1] and identification of charm decay topologies in nuclear emulsions [2–4]. Emulsion based experiments allow highly detailed reconstruction of the event topology such that a background rejection of the order of 10^{-4} can be achieved. The background arises from pions and kaons decaying in flight or hadron interactions without any visible nuclear break-up.

The OPERA experiment was designed to observe $\nu_\mu \to \nu_\tau$ neutrino oscillations in the CNGS beam by the detection of tau leptons produced in ν_τ charged current (CC) interactions. The experiment has been searching for neutrino interactions with one secondary short-lived particle as a signature of the τ lepton. In 2015, OPERA reported the discovery of the ν_τ appearance with a significance of 5.1 σ [5].

An interesting muon-less event with two secondary vertices was identified in the target of the OPERA experiment. Both vertices can be interpreted as heavy particle decay ($c\tau \sim$ 80 μm). According to the Standard Model such an event can originate either from ν_τ CC interaction with charm production or from ν NC interaction with $c\bar{c}$ pair production at the CNGS beam energy. The first one has never been directly observed, while the CHORUS experiment observed three charm pairs produced in ν NC interactions [6]. In OPERA the expected number of such events is smaller than one [7].

In this paper the analysis and interpretation of the interesting event is reported. After a brief description of the OPERA apparatus (section 2), the event measurement and analysis are reported in sections 3 and 4, respectively. The statistical significance of the observation is discussed in section 5.

2 The OPERA experiment

The OPERA detector was located at the LNGS underground laboratory and was exposed to the CERN neutrino to Gran Sasso (CNGS) beam [8]. The experiment profited of a 730 km long baseline; the average neutrino energy was 17 GeV. The beam exposure started in 2008 and ended in 2012 (1.8×10^{20} p.o.t.). In the target fiducial volume 19 505 neutrino interactions were recorded.

2.1 The apparatus

In order to observe and fully reconstruct decay topologies of short-lived particles a spatial resolution at the micrometer scale is required. The OPERA experiment target was made of lead plates inter-spaced with nuclear emulsion films acting as high accuracy tracking devices [9], called Emulsion Cloud Chamber (ECC). The OPERA target was segmented in 150 000 units (bricks) of 57 nuclear emulsion plates alternating with 56 1 mm thick lead plates. The brick cross section is 10.2 cm $\times$ 12.7 cm; its thickness is 7.5 cm corresponding to about 10 radiation lengths. The brick mass is 8.3 kg. The achieved spatial resolution is of $\sim 1\,\mu$m and the angular resolution is of ~ 2 mrad. Charged particle momentum is measured by Multiple Coulomb Scattering (MCS) in the lead plates [10]. Two additional emulsion sheets, called Changeable Sheet doublets (CS), are glued on the brick downstream surface [11].

The active mass of the OPERA target amounted to 1.25 kt. Bricks were hosted in a modular detector made of two identical Super Modules (SM) [9]. Each SM was composed by a target section and a muon spectrometer, as shown in Figure 1. In each SM, the bricks were arranged in 29 vertical walls orthogonal to the beam direction and alternated with electronic detectors [12] consisting of planes of plastic scintillators, called Target Tracker (TT). TT planes were made up of scintillator strips 2.6 cm wide and 1 cm thick arranged perpendicular to each other. The TT system was used to select the brick in which the neutrino interaction occurred. It also provided an estimation of the energy deposited by hadronic and electromagnetic cascades. Spectrometers were designed to measure muon charge and momentum.

2.2 Data taking and event reconstruction

OPERA emulsion analysis is performed by fast automatic scanning systems, based on microscopes equipped with a computer-controlled motorised stage, a dedicated optical system and a camera mounted on top of the optical tube [13–15].

The first step of the event reconstruction is the *location* of the primary neutrino interaction inside the brick [16]. The vertex location procedure in one brick starts from a set of predictions provided by the electronic detectors; then, tracks of secondary particles produced in a neutrino interaction are followed back in the brick, film by film, from the most downstream one to the interaction point where they originate. Whenever a track disappearance hint is detected (the track is not found in three consecutive films), a volume of 1 cm^2 for 5 films upstream and 10 films downstream of the last observed track seg-

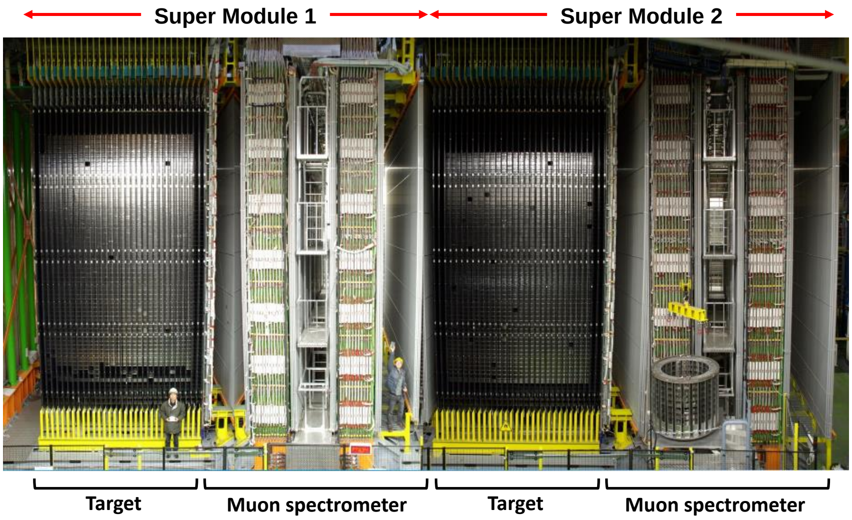

Figure 1: Side view of the OPERA detector; the neutrino beam entered from the left. The upper horizontal lines indicate the position of the two identical supermodules (SM1 and SM2). The target was made of walls filled with bricks interleaved with planes of plastic scintillators (TT).

ment origin is scanned in order to fully reconstruct the event and find any decay candidate through a dedicated decay search procedure.

In this *decay search* procedure [4], secondary vertices are searched for by fine manual measurements of tracks. The hint of a decay topology is the observation of an impact parameter larger than 10 μm, defined as the minimum distance between a track and the reconstructed vertex, excluding low momentum tracks. Decay topologies are classified either as *short* or *long* decays. Short decays are those with a particle decaying in the same lead plate where the primary interaction took place; the remaining ones are long decays. In long decays the signature is the change in slope of a charged particle attached to the primary vertex, without nuclear recoils or knock-on electrons attached to the secondary vertex point.

The precision obtained in the vertex position is affected by particle scattering through lead plates evaluated by Monte Carlo (MC) simulations. Figure 2 shows the impact parameters of reconstructed tracks as a function of the primary vertex depth in lead. If secondary vertices or decays are found, a full kinematical analysis is performed combining the measurements in the nuclear emulsion with data from the electronic detectors.

The appearance of the τ lepton is identified by the detection of its characteristic decay topologies, either in one prong (electron, muon or hadron) or in three prongs. Kinematical selection criteria are applied according to the decay channel [17], shown in Table 1.

The detection and reconstruction efficiencies are evaluated by detailed MC simulations [4].

Table 1: Selection criteria for tau candidates. The value denoted by * is used when a reconstructed EM shower is connected to the kink.

variable	$\tau \to h$	$\tau \to 3h$	$\tau \to \mu$	$\tau \to e$
lepton-tag	No μ or e at the primary vertex			
z_{dec} (μm)	[44; 2600]	< 2600	[44; 2600]	< 2600
p_T^{miss} (GeV/c)	< 1	< 1	–	–
ϕ_{lH} (rad)	$> \pi/2$	$> \pi/2$	–	–
p_T^{2ry} (GeV/c)	$> 0.6\,(0.3)^*$	–	> 0.25	> 0.1
p^{2ry} (GeV/c)	> 2	> 3	> 1	> 1
θ_{kink} (mrad)	> 20	< 500	> 20	> 20
m, m_{min} (GeV/c^2)	–	> 0.5 and < 2	–	–

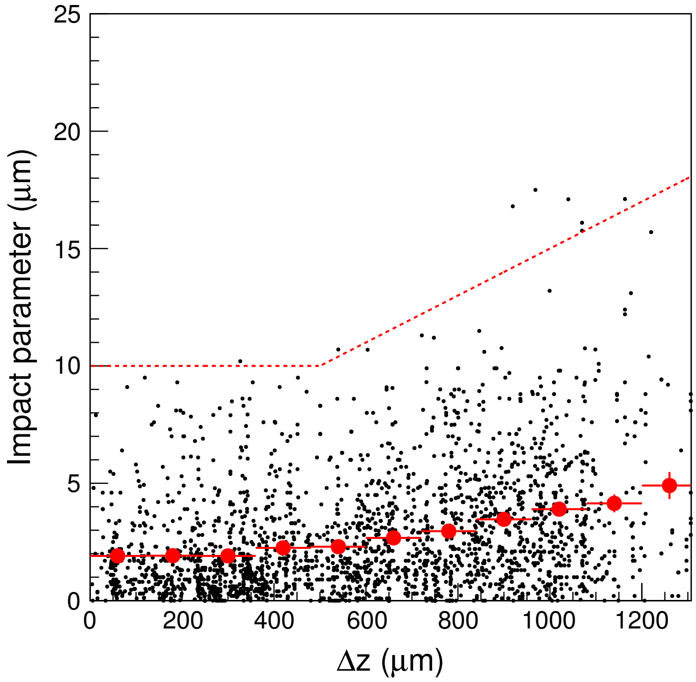

Figure 2: Track impact parameter as a function of the longitudinal distance from the neutrino interaction vertex (2008–2009 data). The red bullets show the average value for each bin. The dotted red line represents the cut applied to select possible short-decay daughter tracks.

3 Event 1114301850

The event 1114301850 was recorded on May 23$^{\text{rd}}$, 2011 in the first SM. The event display is shown in Figure 3: the number of fired TT planes is 9. No muon track is reconstructed therefore the event is tagged as *0-muon*. The energy reconstructed by the TT system is equivalent to 20 ± 6 GeV of hadronic energy released in the lead/emulsion target [12].

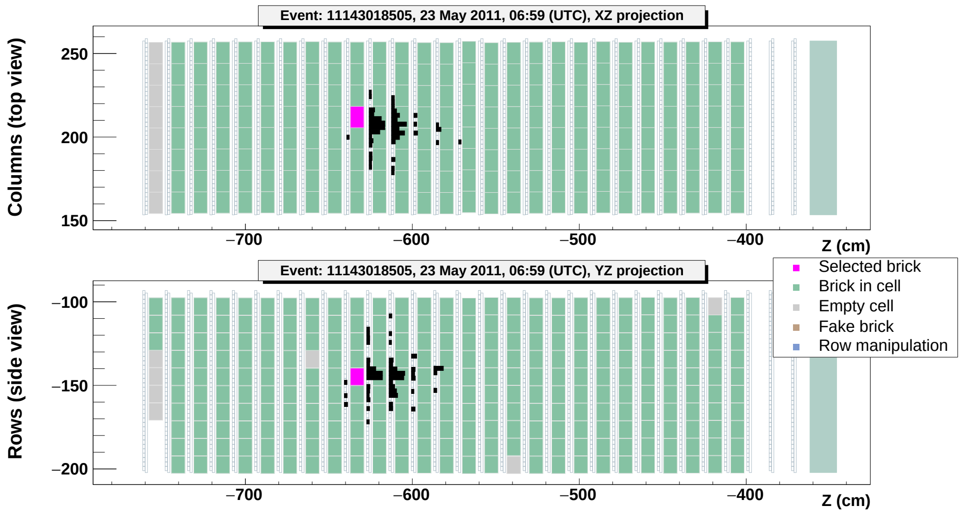

Figure 3: Electronic detector display of the event 1114301850. The neutrino beam direction is along the Z axis entering from the left. Black dots indicates TT hits over threshold and the pink region shows the selected brick (1077152) located in wall 12 of the first SM.

3.1 Data acquisition, event building and reconstruction

The neutrino interaction occurred in brick 1077152, which was extracted from the apparatus for the emulsion film development and measurement. The analysis of the CS doublet reveals a converging pattern of 27 tracks. Out of them, 11 are found also in the brick most downstream plate (plate 57). These tracks are clustered in a region few hundreds micron large, hinting to an electromagnetic activity possibly related to the neutrino interaction. All tracks are followed upstream along the brick; the majority of them are just few emulsion plates long. By visual inspection they are confirmed as electron-positron pairs candidates.

In the location and decay search procedures (see section 2.2), a primary stopping point of 5 tracks is found in plate 32. The reconstructed angular coordinates are reported for each track in Table 2. Following these measurements the neutrino interaction point is located in the lead plate between emulsion plates 31 and 32. Since track 4 impact parameter (IP) is over the 10 μm threshold, a 5-prongs primary vertex topology is discarded. The most probable topology, based on the particle momenta is a double vertex event with the primary neutrino vertex (I) formed by tracks 4, 5, 2 and a secondary vertex (II) formed by tracks 1 and 3. Other configurations have smaller probabilities. Figure 4 shows the superimposition of several emulsion images taken in plate 32; only grains belonging to the event are selected.

Two additional measurements are performed, both allowing a better resolution than the standard one: i) manual measurement with a higher magnification objective and ii) improved automatic image acquisition and analysis. In the first case, the tracks are measured in plate 32 and 33 under a Zeiss 100x objective mounted on the OPERA microscope; thus achieving a 0.3 μm resolution on the position coordinates (X,Y) [18]. In the second case an improved scanning procedure, detailed in [19] is applied. The achieved accuracy in

Table 2: Slopes of tracks at plate 32 and their impacts parameters (IPs), evaluated assuming a single vertex topology and a two vertices one. The single vertex, V_0 has coordinates $x = 15083.4\,\mu$m, $y = 59151.5\,\mu$m and $z = -32999.0\,\mu$m. Vertices V_I and V_{II} are defined in Table 3.

			One Vertex IP (μm)	**Two vertices IP** (μm)	
Track	θ_x (rad)	θ_y (rad)	w.r.t. V_0	w.r.t. V_I	w.r.t. V_{II}
1	-0.230	-0.275	8.3	36.2	0.1
2	0.121	-0.144	8.8	1.0	6.5
3	0.349	-0.036	4.8	25.9	0.1
4	-0.003	0.088	13.0	1.5	20.4
5	-0.003	-0.025	5.1	2.2	9.6

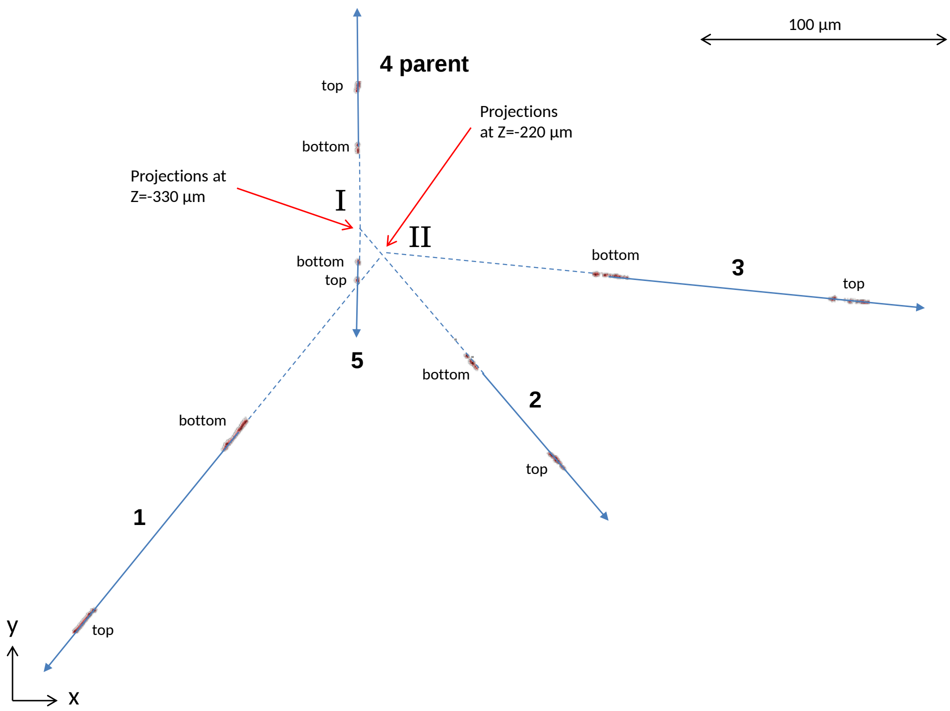

Figure 4: Superimposition of several tomographic emulsion images taken at different depth in plate 32; images are processed to remove fog and Compton electron grains and to show only grains related to the events. Each track is composed by two *groups* of clustered grains because OPERA emulsions have two sensitive layers (*top* and *bottom*).

3D cluster finding is better than one micron and a 3D tracking algorithm is applied.

The primary vertex is located 581.8 μm upstream with respect to the top emulsion layer of plate 32. The flight length of a neutral particle originated at the primary vertex with angles (0.0862; 0.0774) mrad and decaying at the secondary vertex, would be 103.2 μm.

Track 4 (*parent*) shows a kink topology (vertex III) between plates 32 and 33. The minimum distance between track 4 and track 6 (*daughter*) emerging from the kink, is $(0.9 \pm 0.4)\,\mu$m. The kink angle is (95 $\pm$ 2) mrad; parent flight length is $(1174 \pm 5)\,\mu$m.

All tracks reconstructed at plates 32 and 33 are followed down in the brick in order to estimate their momenta and to asses that they belong to the event by confirming their presence in the CS doublet. A scheme of the full event is shown in Figure 5.

Track 2 stops at plate 34; track 3 undergoes a re-interaction at plate 53, while track 1, 5 and 6 reach the CS plates. The coordinates of the three vertices are listed in Table 3.

By the decay search procedure two e^+e^- pairs are identified in plates 35 (γ_1) and 41 (γ_2). An innovative procedure developed to identify and reconstruct the electromagnetic showers [19] is applied. An image data taking with 1 micron Z pitch is performed in a cone of 400 mrad aperture around the slope of the primary photon, starting from plate 31 down to plate 57 in the brick. All tracks in the volume are reconstructed using the 3D tracking algorithm. The main features of the reconstructed showers are listed in Table 4 and shown in figure Figure 6.

The most downstream shower tracks are reconstructed in the CS plates, confirming that the primary photons are related to the primary neutrino interaction. Their parents are not relevant for the analysis described in the section 4 which takes into account only the total visible electromagnetic energy. The accuracy of the reconstruction procedure allows to establish that γ_1 points to the kink, while γ_2 may emerge from any vertex (I, II or III).

A dedicated scanning system was used [21] to search for nuclear fragments at each vertex, within $|\tan\theta| < 3$ acceptance window. No nuclear fragment was detected.

3.2 Kinematics

Momenta of tracks 1, 3, 5, 6 are estimated by the MCS method. The alignment accuracy is evaluated from the angular and position resolution of a sample of penetrating tracks reconstructed in the scanned volume. All measurements are performed on high resolution image files. The achieved angular and position resolution is $3.4/\sqrt{2}$ mrad and $0.8/\sqrt{2}\,\mu$m respectively. Results are shown in Table 5.

Being track 2 measured only in three emulsion plates, its momentum can not be estimated by MCS. An estimation of the momentum is obtained by the NIST code [22] and yields to $\beta < 0.5$, whatever the mass of particle 2. However, this evaluation is not compatible with the visible energy loss in emulsion for this track, which is identified as a m.i.p. by counting the developed grains along the track. Therefore, a different estimation is performed considering absorption processes which have a resonance at a kinetic energy

Table 3: Position inside the brick of the reconstructed vertices. The z coordinate is evaluated with respect to the downstream side of the brick (plate 57).

Vertex ID	Parent	Daughters	x (μm)	y (μm)	z (μm)
I (primary)	-	2, 4, 5, neutral	15077.0	59157.9	-33081.8
II (secondary)	neutral	1, 3	15085.9	59149.9	-32979.2
III (kink)	4	6	15073.9	59262.4	-31926.4

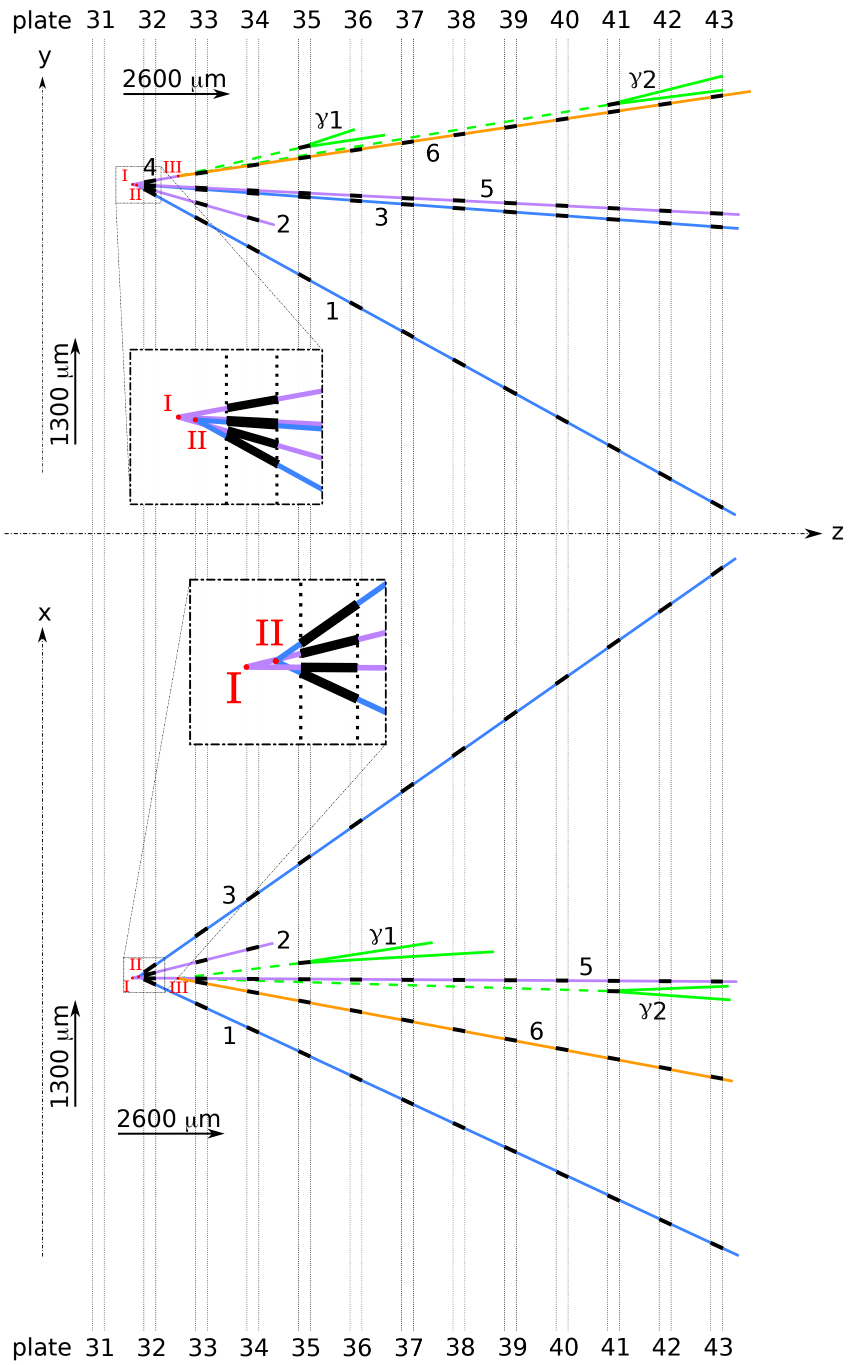

Figure 5: Projection of the event in the YZ (upper plot) and XZ (down plot) planes. Energy deposits measured in a single emulsion films are represented in black, while global reconstructed tracks are represented using colored lines: purple for tracks coming from the primary vertex (I), blue for tracks coming from vertex II and orange for the daughter of vertex III. For photons, only the first electron-positron pair is shown (black).

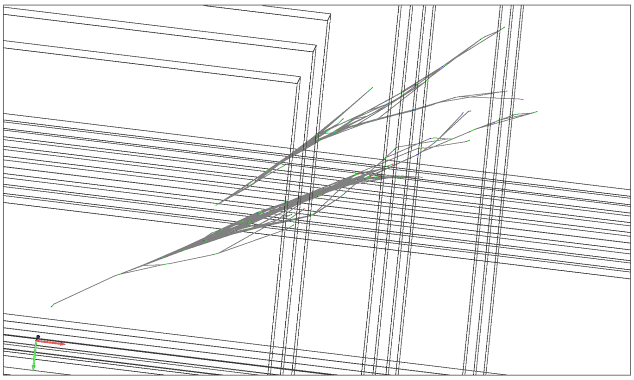

Figure 6: Reconstruction of the electromagnetic showers associated to the event.

of about 200 MeV, for pions in every material [23, 24]. In this region, especially for high A nuclei, the absorption cross section is up to ~ 40 % of the total cross section. From these arguments, the momentum estimation for track 2 is (0.31 ± 0.08) GeV/c. This is the initial momentum of a pion which is absorbed after crossing 2 mm of lead and that has a kinetic energy of about 200 MeV when absorbed. The uncertainty is evaluated assuming a uniform kinetic energy distribution: the minimum is the kinetic energy such that $\beta > 0.7$; while the maximum is 300 MeV, which is the endpoint of the absorption peak.

The energies of the electromagnetic showers, γ_1 and γ_2, are estimated by counting the electron tracks belonging to each shower. The procedure is calibrated with MC simulations, taking into account also background tracks in emulsions. The results are $E_{\gamma_1} = (7.2 \pm 1.7)$ GeV and $E_{\gamma_2} = (5.3 \pm 2.2)$ GeV.

In conclusion, event 1114301850 is identified as a neutrino interaction with two secondary vertices: vertex II has a 2-prong topology while Vertex III is a kink originated by a primary charged particle. The invariant mass at each vertex are reported in Table 6.

Table 4: Electromagnetic showers features. Reconstructed energies were estimated counting the tracks multiplicity [20].

Shower ID	γ_1	γ_2
Starting plate	35	41
θ_x (rad)	0.050	0.011
θ_y (rad)	0.122	0.085
$\mathrm{IP_I}$ (μm)	30 ± 22	40 ± 23
$\mathrm{IP_{II}}$ (μm)	28 ± 22	40 ± 23
$\mathrm{IP_{III}}$ (μm)	8 ± 8	40 ± 11
Opening angle (rad)	0.027	0.029
Energy (GeV)	7.1 ± 1.7	5.3 ± 2.2

Table 5: Particles momenta reconstructed by the multiple Coulomb scattering method.

Track ID	p best fit (GeV/c)	68 % p range (GeV/c)
1	2.1	[1.6 ; 3.1]
3	4.3	[3.1 ; 7.1]
5	0.54	[0.45 ; 0.68]
6 (daughter)	2.7	[2.1 ; 3.7]

Table 6: Secondary vertices invariant masses and minimum invariant masses. The differences are evaluated too, $\Delta \equiv M_{min} - M$. Due to the correlation between the two distributions, the errors are relatively small.

Vertex ID	Invariant Mass M (GeV/c^2)	Minimum Invariant Mass M_{min} (GeV/c^2)	Difference Δ (GeV/c^2)
II	1.8 ± 0.5	2.5 ± 0.8	0.7 ± 0.4
III (kink)	0.9 ± 0.1	1.2 ± 0.2	0.3 ± 0.1

4 Event analysis

The standard OPERA analysis does not include events with double-decay topology. Associated charm production is taken into account only as a background in the tau search, assuming the identification of just one decay vertex.

According to the standard OPERA analysis neither of the two decays can be classified as a tau candidate [7, 17]. In particular, the vertex III (kink) matches all selection criteria except for the daughter transverse momentum (p_T) which should be > 0.300 GeV/c, while the event kink daughter has $p_T = (0.24 \pm 0.07)$ GeV/c.

Therefore a non-standard new analysis is necessary for a more accurate classification of event 1114301850. In CNGS kinematic conditions, two short-lived particle decays can be produced by the following processes(Figure 7):

- ν_τ CC interaction with charm production;
- ν NC interaction with $c\bar{c}$ pair production;

Other processes faking this topology are:

- ν_μ CC interaction with a mis-identified muon and two secondary interactions.
- ν_μ CC interaction with single charm production, a mis-identified muon and one secondary interaction;
- ν NC interaction with two secondary interactions;
- ν_τ CC interaction with one secondary interaction;

A secondary interaction can be either i) hadronic interaction of a final state particle, ii) short decay of pions or kaons, or iii) large angle Coulomb scattering by hadrons or mis-identified muons.

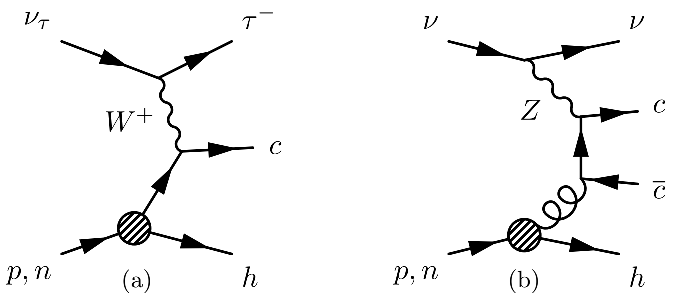

Figure 7: Leading Feynman diagrams for the production of two prompt short decaying particles: (a) tau charm production in CC interaction and (b) charm pair production in NC interaction .

The new analysis is based on the distributions of kinematical variables obtained through a dedicated MC production. Neutrino interactions are generated using GENIE [25] besides charm pair production, which is simulated using HERWIG [26]. Due to the high multiplicity of event 1114301850, only DIS interactions are taken into account. In total, about 300 million events are generated.

Particles from neutrino interactions are propagated in few cubic centimeter volumes of the OPERA brick using the Geant4 framework [27, 28], assuming that the primary vertex has the same depth in lead as the one estimated for event 1114301850. The MCS is taken into account using a parametrization based on the standard OPERA MC. The hadronic interaction simulations are validated with dedicated test beam data [29].

For each process, the number of expected events is normalized to the 12 352 observed CC events with a primary vertex in the target section of the OPERA experiment considering the shape of the CNGS neutrino flux [8], the oscillation probabilities and the cross section. The vertex location efficiency is determined according to a data driven parameterization. The efficiencies related to the electronic detectors (brick selection, muon identification, muon momentum estimation) are evaluated using the standard OPERA MC with a parameterization based on the hadronic energy and muon momentum.

Simulated events are selected regardless of the multiplicity at the primary vertex by requiring:

- no muon nor electron reconstructed at the primary vertex;
- a one prong-like secondary vertex (1pr-like);
- a two prong-like secondary vertex (2pr-like);
- no fragments at any vertex.

Moreover, the 1pr-like daughter has to be a charged track but not a muon, neither an electron nor a positron. The 1pr-like parent is required to be charged and crossing at least one emulsion plate. No kinematical cuts are applied.

The total number of expected events matching the topology of event 1114301850 is ~ 0.1; the details for each simulated process are given in Table 7.

Table 7: Expected events with a two secondary-vertices topology as selected by the analysis.

Sample	Expected events (10^{-3})
ν_τ CC + charm	44.5 ± 0.1
ν NC + $c\bar{c}$ pair	12.59 ± 0.02
ν_μ CC + two 2ry	4.0 ± 0.5
ν_μ CC + charm + 2ry	20.5 ± 0.5
ν NC + two 2ry	3.8 ± 0.3
ν_τ CC +2ry	9.0 ± 0.1
Total	94.4

A multivariate analysis is applied on selected events and the signal the signal to background discrimination is based on 12 kinematic variables:

- the *total EM energy*, that is the sum of the visible photon energy, regardless of the photon origin vertex;
- the *transverse angle* φ between the parents of the 1pr-like and 2pr-like vertices;
- the *missing transverse momentum* at primary vertex with respect to the beam direction;
- the *hadronic momentum*, i.e. the sum of the primary track momenta excluding the two parents;

for the 1pr-like vertex:

- the *daughter's momentum*;
- the *daughter's transverse momentum* with respect to the parent direction;
- the *flight length*.
- the *kink* angle between parent and daughter;

for the 2pr-like vertex:

- the total *daughters' momentum*;
- the total *daughters' transverse momentum* with respect to the parent direction;
- the *flight length*.
- the *invariant mass* of the charged daughters.

In order to find the best method for the discrimination, several algorithms are tested: an Artificial Neural Networks (ANN) method [30], two kinds of Boost Decision Trees [31] and the Fisher Discriminant [32]. The optimal one turns out to be the ANN, whose output variable distribution is shown in Figure 8.

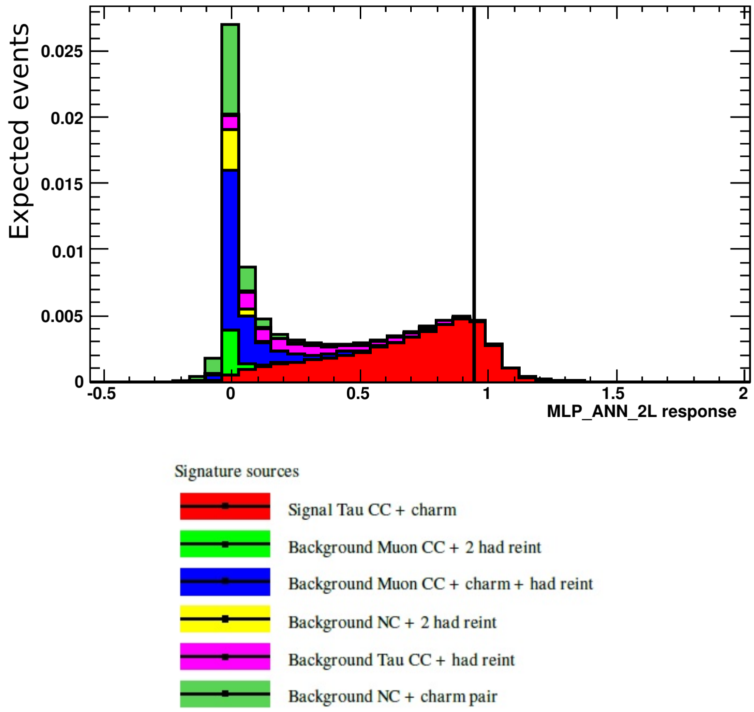

Figure 8: Distribution of the ANN output variable. The weighted contribution of each source of Table 7 is shown with a different color. The vertical black line represents the ANN output for the event 1114301850.

5 Significance

As shown in Figure 8, according to the multivariate analysis the event can be classified as a ν_τ CC interaction with charm production with rather high probability. The significance of the result is evaluated using RooFit/RooStats libraries [33] provided by the ROOT framework [34].

The observable of the model is the ANN output variable x whose distribution, normalized to the expected number of events, is shown in Figure 8. Its shape is obtained by the sum of the contributions of each process reported in Table 7. In order to evaluate the significance, a parameter μ, the signal strength, is introduced such that the background only hypothesis corresponds to $\mu = 0$, while $\mu = 1$ represents the background plus the expected signal model. The likelihood can be written as:

$$\mathcal{L}(\mu|x) = \sum_i n_i b_i(x) + \mu \cdot n_s s(x) \tag{5.1}$$

where $s(x)$ and $b_i(x)$ are the signal and backgrounds PDFs, respectively; n_i and n_s the expected number of events.

Systematic effects are introduced as scale factors, f_j, different for each process. Scale factors f_j depend on nuisance parameters σ_k distributed according to their PDFs, g_k. Some nuisance parameters are specifically defined for a particular process, while others are common to several contributions. The first nuisance parameter is a normalization factor, σ_N. The normalization is dominated by the CNGS flux uncertainty, which is about 20 % [8]. Another source of uncertainty are cross sections of two processes not observed in the OPERA experiment: NC interactions with charm pair production and ν_τ CC interactions with single charm. These uncertainties are assumed to be 20 %. The systematic cross section error of ν_τ CC interactions without charm estimated from [35] is 6 % for ν_τ in the few tens of GeV range. The uncertainty associated to the hadron re-interaction is 30 %, according to data-MC comparisons based on test beam results [29].

Each nuisance parameter distribution g_k depends on some constant parameters as the range boundaries or other PDF parameters like Gaussian variances. These are different for each g_k and they are labeled $\hat{\boldsymbol{\sigma}}_k$. Hence, nuisance parameters distributions are identified as $g_k(\sigma_k|\hat{\boldsymbol{\sigma}}_k)$.

Including systematics, the likelihood can be expressed as:

$$\mathcal{L}(\mu, \boldsymbol{\sigma}|x) = \left[\sum_{i \in B} f_i(\boldsymbol{\sigma})\, n_i b_i(x) + \mu f_s(\boldsymbol{\sigma})\, n_s s(x)\right] \prod_k g_k(\sigma_k|\hat{\boldsymbol{\sigma}}_k) \tag{5.2}$$

where $\boldsymbol{\sigma}$ indicates the whole set of nuisance parameters.

The test statistic used for the significance evaluation is the profile likelihood ratio [36, 37]. A sample of MC pseudo-experiments is generated according to the background only PDF, in order to get the test statistic distribution (Figure 9). In each pseudo-experiment, nuisance parameters are varied according to their PDFs. Under the background only hypothesis, the probability of data being less likely or equal to the observed event is $(2.6 \pm 0.2) \times 10^{-4}$. Therefore, the absence of ν_τCC interaction with charm production can be excluded with a significance of 3.5 standard deviations.

The most likely interpretation is that vertex II is originated by a charm decay and vertex III by tau decay into an hadron.

6 Conclusions

A neutrino interaction event was observed in the OPERA target having a rare topology: two secondary vertices within about 1 mm from the primary one were observed. Such topology could arise from ν_τ interaction with charm production and ν NC interaction with double charm production. Dedicated scanning and analysis procedures were thus performed for this event that was not considered in the original OPERA proposal.

The event turned out to be very likely a ν_τ CC interaction with charm production with a significance of about $3.5\,\sigma$.

Acknowledgments

We acknowledge CERN for the successful operation of the CNGS facility and INFN for the continuous support given to the experiment through its LNGS laboratory. We acknowledge funding from our national agencies: Fonds de la Recherche Scientifique-FNRS and Institut Inter Universitaire des Sciences Nucleaires for Belgium; MoSES for Croatia; CNRS

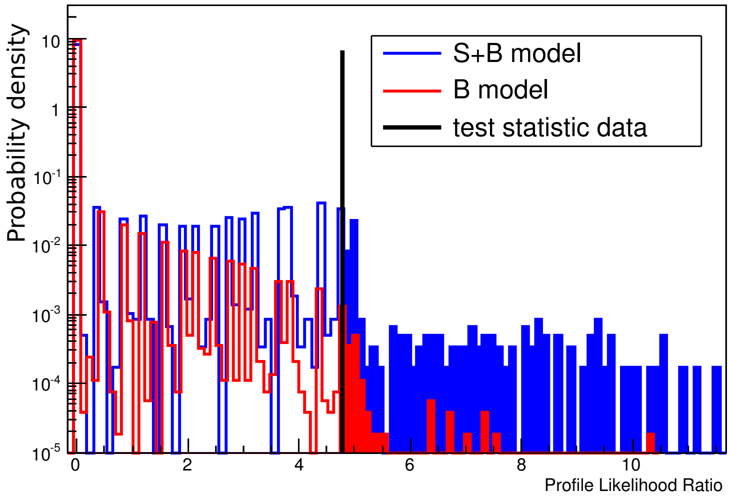

Figure 9: Expected distributions of the test statistic (profile likelihood ratio) obtained by pseudo-experiments under the background only hypothesis (*B model*, $\mu = 0$) and signal plus background hypothesis (*S+B model*, $\mu = 1$). The black line indicates the value obtained by applying the test statistic on the observed data.

and IN2P3 for France; BMBF for Germany; INFN for Italy; JSPS, MEXT, the QFPU-Global COE program of Nagoya University, and Promotion and Mutual Aid Corporation for Private Schools of Japan for Japan; SNF, the University of Bern and ETH Zurich for Switzerland; the Russian Foundation for Basic Research (Grant No. 12-02-12142 ofim), the Programs of the Presidium of the Russian Academy of Sciences (Neutrino Physics and Experimental and Theoretical Researches of Fundamental Interactions), and the Ministry of Education and Science of the Russian Federation for Russia, the National Research Foundation of Korea Grant (No. NRF-2013R1A1A2061654) for Korea; and TUBITAK, the Scientific and Technological Research Council of Turkey for Turkey. We thank the IN2P3 Computing Centre (CC-IN2P3) for providing computing resources.

References

[1] P. Vilain et al., *Leading-order QCD analysis of neutrino-induced dimuon events*, *The European Physical Journal C - Particles and Fields* **11** (1999) 19–34.

[2] A. Kayis-Topaksu et al., *Measurement of charm production in neutrino charged-current interactions*, *New J. Phys.* **13** (2011) 093002, [1107.0613].

[3] N. Ushida, T. Kondo, G. Fujioka, H. Fukushima, Y. Takahashi, S. Tatsumi et al., *Experimental details on lifetime measurements of neutrino-produced charmed particles in a tagged emulsion spectrometer*, *Nuclear Instruments and Methods in Physics Research* **224** (1984) 50–64.

[4] N. Agafonova, A. Aleksandrov, A. Anokhina, S. Aoki, A. Ariga, T. Ariga et al., *Procedure for short-lived particle detection in the OPERA experiment and its application to charm decays*, *Eur. Phys. J. C* **74** (2014) 2986.

[5] OPERA collaboration, N. Agafonova, A. Aleksandrov, A. Anokhina, S. Aoki, A. Ariga, T. Ariga et al., *Discovery of τ neutrino appearance in the CNGS neutrino beam with the OPERA experiment*, Phys. Rev. Lett. **115** (9, 2015) 121802.

[6] CHORUS collaboration, A. Kayis-Topaksu et al., *Associated charm production in neutrino-nucleus interactions*, Eur. Phys. J. **C52** (2007) 543–552, [0708.2820].

[7] M. Guler et al., *OPERA: An appearance experiment to search for $\nu_\mu \longleftrightarrow \nu_\tau$ oscillations in the CNGS beam*, *Experimental proposal CERN-SPSC-2000-028* (2000) .

[8] R. Bailey, J. L. Baldy, A. E. Ball, P. Bonnal, M. Buhler-Broglin, C. Dtraz et al., *The CERN Neutrino beam to Gran Sasso (NGS)*, Tech. Rep. CERN-SL-99-034-DI. INFN-AE-99-05, CERN, Geneva, Jun, 1999.

[9] Agafonova, N and Anokhina, A and Aoki, S and Ariga, A and Ariga, T and Arrabito, L and Autiero, D and Badertscher, A and Bagulya, A and Greggio, F Bersani and others, *The detection of neutrino interactions in the emulsion/lead target of the OPERA experiment*, *Journal of Instrumentation* **4** (2009) P06020.

[10] OPERA collaboration, N. Agafonova et al., *Momentum measurement by the Multiple Coulomb Scattering method in the OPERA lead emulsion target*, New J. Phys. **14** (2012) 013026, [1106.6211].

[11] OPERA collaboration, A. Anokhina et al., *Emulsion sheet doublets as interface trackers for the OPERA experiment*, JINST **3** (2008) P07005, [0804.1985].

[12] OPERA collaboration, N. Agafonova et al., *Study of neutrino interactions with the electronic detectors of the OPERA experiment*, New J. Phys. **13** (2011) 053051, [1102.1882].

[13] K. Morishima and T. Nakano, *Development of a new automatic nuclear emulsion scanning system, S-UTS, with continuous 3D tomographic image read-out*, *Journal of Instrumentation* **5** (2010) P04011.

[14] C. Bozza, N. D'Ambrosio, G. De Lellis, M. De Serio, F. Di Capua, A. Di Crescenzo et al., *An integrated system for large scale scanning of nuclear emulsions*, *Nuclear Instruments and Methods in Physics Research Section A: Accelerators, Spectrometers, Detectors and Associated Equipment* **703** (2013) 204–212.

[15] L. Arrabito, E. Barbuto, C. Bozza, S. Buontempo, L. Consiglio, D. Coppola et al., *Hardware performance of a scanning system for high speed analysis of nuclear emulsions*, *Nuclear Instruments and Methods in Physics Research Section A: Accelerators, Spectrometers, Detectors and Associated Equipment* **568** (2006) 578 – 587.

[16] N. Agafonova, A. Anokhina, S. Aoki, A. Ariga, T. Ariga, L. Arrabito et al., *The detection of neutrino interactions in the emulsion/lead target of the OPERA experiment*, *Journal of Instrumentation* **4** (2009) P06020.

[17] N. Agafonova, A. Aleksandrov, O. Altinok, M. Ambrosio, A. Anokhina, S. Aoki et al., *Observation of a first $\nu\tau$ candidate event in the OPERA experiment in the CNGS beam*, *Physics Letters B* **691** (2010) 138–145.

[18] L. Arrabito et al., *Hardware performance of a scanning system for high speed analysis of nuclear emulsions*, Nucl. Instrum. Meth. **A568** (2006) 578–587, [physics/0604043].

[19] F. Laudisio, *Proposta di ricostruzione di Sciami Elettromagnetici in emulsione con particolare riferimento all'esperimento OPERA*,

operaweb.lngs.infn.it/Opera/ptb/theses/theses/Laudisio-Fulvio-Master-thesis-Feb2015.pdf (2015) .

[20] C. Sirignano et al., *Electromagnetic showers study by detailed image analysis*, *indico.cern.ch/event/365741/session/4/contribution/3/attachments/727206/997866/shower_sirignano_15_3_2015.pdf* (2015) .

[21] A. Alexandrov, V. Tioukov and M. Vladymyrov, *Further progress for a fast scanning of nuclear emulsions with large angle scanning system*, *Journal of Instrumentation* **9** (2014) C02034.

[22] M. J. Berger, J. Coursey, M. Zucker and J. Chang, *Stopping-power and range tables for electrons, protons, and helium ions*, 2009.

[23] D. Ashery, I. Navon, G. Azuelos, H. K. Walter, H. J. Pfeiffer and F. W. Schlepütz, *True absorption and scattering of pions on nuclei*, *Phys. Rev. C* **23** (5, 1981) 2173–2185.

[24] R. A. Giannelli, B. G. Ritchie, J. M. Applegate, E. Beck, J. Beck, A. O. Vanderpool et al., *Multiproton final states in positive pion absorption below the* $\Delta(1232)$ *resonance*, *Phys. Rev. C* **61** (4, 2000) 054615.

[25] C. Andreopoulos et al., *The GENIE Neutrino Monte Carlo Generator*, *Nucl. Instrum. Meth.* **A614** (2010) 87–104, [0905.2517].

[26] G. Corcella, I. G. Knowles, G. Marchesini, S. Moretti, K. Odagiri, P. Richardson et al., *HERWIG 6: An Event generator for hadron emission reactions with interfering gluons (including supersymmetric processes)*, *JHEP* **01** (2001) 010, [hep-ph/0011363].

[27] S. Agostinelli, J. Allison, K. Amako, J. Apostolakis, H. Araujo, P. Arce et al., *Geant4–a simulation toolkit*, *Nuclear Instruments and Methods in Physics Research Section A: Accelerators, Spectrometers, Detectors and Associated Equipment* **506** (2003) 250 – 303.

[28] J. Allison, K. Amako, J. Apostolakis, H. Araujo, P. Dubois, M. Asai et al., *Geant4 developments and applications*, *Nuclear Science, IEEE Transactions on* **53** (2, 2006) 270–278.

[29] H. Ishida, T. Fukuda, T. Kajiwara, K. Kodama, M. Komatsu, T. Matsuo et al., *Study of hadron interactions in a lead–emulsion target*, *Progress of Theoretical and Experimental Physics* **2014** (2014) 093C01.

[30] A. Hoecker, P. Speckmayer, J. Stelzer, J. Therhaag, E. von Toerne and H. Voss, *TMVA: Toolkit for Multivariate Data Analysis*, *PoS* **ACAT** (2007) 040, [physics/0703039].

[31] Y. Freund and R. E. Schapire, *A decision-theoretic generalization of on-line learning and an application to boosting*, *Journal of Computer and System Sciences* **55** (1997) 119 – 139.

[32] R. A. Fisher, *The use of multiple measurements in taxonomic problems*, *Annals of eugenics* **7** (1936) 179–188.

[33] W. Verkerke and D. P. Kirkby, *The RooFit toolkit for data modeling*, *eConf* **C0303241** (2003) MOLT007, [physics/0306116].

[34] R. Brun and F. Rademakers, *ROOT – An object oriented data analysis framework*, *Nuclear Instruments and Methods in Physics Research Section A: Accelerators, Spectrometers, Detectors and Associated Equipment* **389** (1997) 81 – 86.

[35] Y. S. Jeong and M. H. Reno, *Tau neutrino and antineutrino cross sections*, *Phys. Rev.* **D82** (2010) 033010, [1007.1966].

[36] G. Ranucci, *The profile likelihood ratio and the look elsewhere effect in high energy physics*, *Nuclear Instruments and Methods in Physics Research Section A: Accelerators, Spectrometers, Detectors and Associated Equipment* **661** (2012) 77 – 85.

[37] G. Cowan, K. Cranmer, E. Gross and O. Vitells, *Asymptotic formulae for likelihood-based tests of new physics*, *The European Physical Journal C* **71** (2011) 1–19.